Volume 46(9): 985–992, 1998
The Journal of Histochemistry & Cytochemistry
http://www.jhc.org

ARTICLE

The Size of Sites Containing SR Proteins in Human Nuclei: Problems Associated with Characterizing Small Structures by Immunogold Labeling

Francisco J. Iborra and Peter R. Cook

Sir William Dunn School of Pathology, University of Oxford, Oxford, United Kingdom

SUMMARY Some SR proteins are associated with eukaryotic transcripts as they move from synthetic sites (transcription "factories"), through downstream sites, to nuclear pores. Downstream sites can also be isolated as large nuclear ribonucleoprotein particles of ~200 S (diameter ~50 nm). In ultrathin sections of HeLa nuclei, indirect immunogold labeling with a specific antibody gives many small clusters of ~10 gold particles (diameter 50–80 nm). We gauged errors in estimating the diameter of underlying structures marked by immunogold probes (lengths ~20 nm). We examined systematically how probe dimensions affected cluster diameter. Probes contained one to three immunoglobulin molecules, sometimes a protein A molecule, and a gold particle of 5–15 nm. We found that (a) immunolabeling particles were tightly packed, (b) reducing particle size by 5 nm reduced cluster diameter by 10 nm, (c) reducing the number of immunoglobulins in the immunolabeling sandwich from three to two reduced cluster diameter by ~4 nm, (d) replacing the last immunoglobulin in a sandwich with protein A increased diameter by ~7 nm and led to a peripheral concentration of particles, and (e) increasing the number of layers in the sandwich increased sensitivity. Assuming that underlying structures had diameters of 50 nm, we find that errors ranged from −20% to +50%. **(J Histochem Cytochem 46:985–992, 1998)**

KEY WORDS
immunoelectron microscopy
immunogold labeling
LR White
resolution

Antibodies attached to gold particles are widely used to mark antigens lying on the surface of sections. The antibody binds specifically to the antigen and the dense gold particle can be seen easily in the electron microscope (Bendayan 1995). The accuracy with which an antigen can be located depends on various factors, including the dimensions of the immunolabeling complex. For example, sandwiches containing two molecules of immunoglobulin and one of protein A (lengths of ~9, ~9, and ~5 nm, respectively) are commonly used to label subcellular structures, so that an immunolabeling particle can, in principle, lie ~23 nm away from the antigen it marks. In practice, many studies have shown that resolution is usually better than this (reviewed by Griffiths 1993). The most detailed studies concern antigens embedded in membranes. As expected, most immunolabeling particles lie over the membrane, but some are found to one or the other side at a distance that depends on the number of antibodies in the sandwich. We now address a related problem: determining the true size of small spherical structures with diameters two- to threefold that of the probe.

We illustrate the problem using a specific example, SR sites in the nucleoplasm of mammalian cells. These sites are defined using a monoclonal antibody (MAb) that recognizes a phosphorylated subset of the SR family of proteins (Roth et al. 1990). After indirect immunogold labeling, each site is seen as a small cluster of ~10 gold particles with a major axis of ~65 nm (Iborra et al. in press). [SR proteins are splicing factors; they are so named because they have serine- and arginine-rich carboxy terminal domains (Zahler et al. 1992; Kramer 1996).] Most SR sites contain newly made transcripts in transit from primary transcription sites to nuclear pores (Iborra et al. in press; Jackson et al. in press). They can be isolated on sucrose gradi-

Correspondence to: Peter R. Cook, Sir William Dunn School of Pathology, Univ. of Oxford, South Parks Road, Oxford OX1 3RE, UK. E-mail: Peter.Cook@Path.OX.AC.UK.

Received for publication January 21, 1998; accepted April 8, 1998 (8A4579).

0022-1554/98/$3.30

ents as large nuclear ribonucleoprotein particles of ~200 S. A low-resolution structure indicates that these 200-S particles are tetramers with an overall diameter of ~50 nm (Yitzhaki et al. 1996; Sperling et al. 1997). Therefore, it is possible to compare the dimensions of SR sites (seen indirectly as clusters of gold particles on sections) with those observed directly in the isolated particles. This, in turn, should enable us to gauge the errors in estimating diameters by immunogold labeling.

Several interrelated factors complicate analysis. First, SR sites with diameters of ~65 nm are not much larger than the smallest probe in everyday use (i.e., an immunoglobulin with a length of 9 nm conjugated with a 5-nm particle). Second, they can be detected efficiently only by using two or more antibody layers, but then the probe has a size close to that of the site under analysis. Third, sites are so small that they become saturated with ~10 immunolabeling particles. Analysis must be conducted at or close to saturation levels, because slight reductions inevitably lead to a significant underestimate of diameter. This follows because halving the number of particles over a structure from a saturation level of 10 to 5 has a significant effect on the area occupied by the cluster. Fourth, stereological analysis should (but usually does not) take into account the probabilistic effects of dealing with so few particles. We correlated changes in the number of layers in the immunolabeling sandwich and size of gold particle with the observed diameter of the cluster. We also investigated how replacement of one immunoglobulin in the sandwich with protein A affected labeling. We hope that these results will be of general use to others trying to gauge errors in estimating the diameter of underlying structures using probes with dimensions close to that of the structure being analyzed.

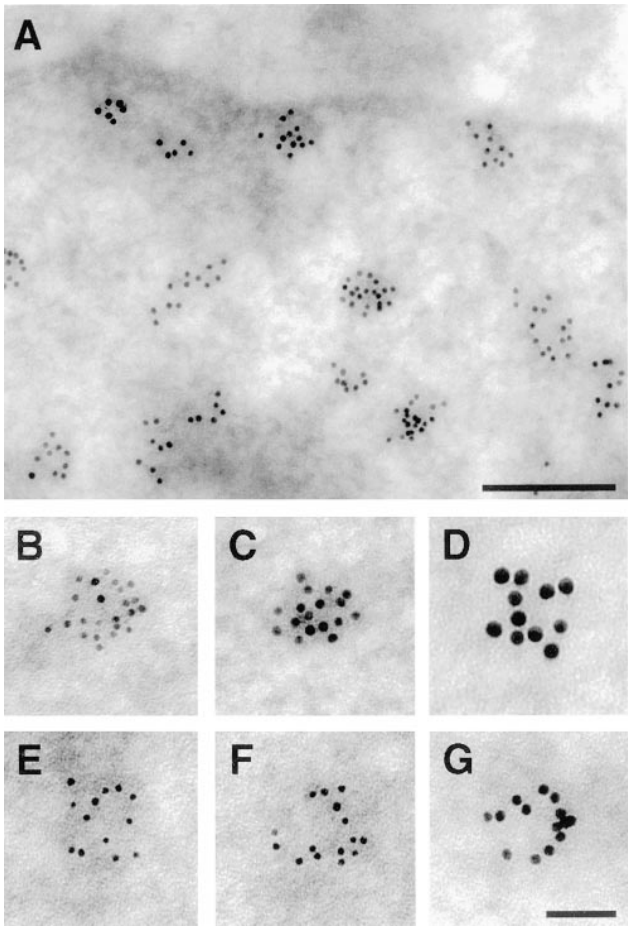

Figure 1 SR antigens are clustered in HeLa nuclei. Cells were fixed, embedded in LR white, and the surface of ultrathin sections immunogold labeled as indicated. Particles are distributed throughout clusters in **A–E** and at the periphery in **F** and **G**. (**A**) Anti-SR, rabbit anti-mouse Ig, and goat anti-rabbit conjugated with 10-nm particles; particles lie in clusters over the nucleus (bottom), but not cytoplasm (top). (**B–D**) Anti-SR, rabbit anti-mouse Ig, and goat anti-rabbit conjugated with 5-(**B**), 10-(**C**), or 15 (**D**)-nm particles. (**E**) Anti-SR, goat anti-mouse conjugated with 5-nm particles. (**F,G**) Anti-SR, rabbit anti-mouse Ig, and protein A conjugated with 5-(**F**) or 9 (**G**)-nm particles. Bars: **A** = 200 μm; **B–G** = 50 μm.

Materials and Methods

Immunolabeling

Phosphorylated SR antigens were detected using an MAb produced by cell line m104 (ATCC CRL-2067; Rockville, MD) (Roth et al. 1990). Antibodies directly conjugated with gold particles included goat anti-biotin, goat anti-rabbit IgG, and goat anti-mouse IgG (British BioCell; Cardiff, UK). Mouse anti-biotin and rabbit anti-mouse IgG were from Jackson Laboratories (Stratech Laboratories; Luton, UK), rabbit anti-mouse IgM (μ region) was from Cappel Laboratories (West Chester, PA), protein A–gold (5 nm) was from BioCell, and protein A–gold (9 nm) was made as described by Iborra et al. (1996).

For Figure 1, suspension cultures of HeLa cells were pelleted, washed with PBS, and fixed (10 min, 0C) in 4% paraformaldehyde in 250 mM Hepes (pH 7.4) and postfixed (50 min; room temperature) in 8% paraformaldehyde in 250 mM Hepes. After washing successively in PBS, 0.02 M glycine in PBS, and then PBS, cells were dehydrated in ice-cold ethanol, embedded in LR White (polymerization 5 hr at 56C; London Resin Company, Reading, Berks, UK) and ultrathin sections on nickel grids immunolabeled. Unspecific binding was blocked by preincubation (30 min) in PBS (pH 8.2) with 0.1% Tween 20 and 1% BSA (PBTB buffer). Next, sections were incubated (2 hr) with the anti-SR MAb (1:100 dilution of supernatant) in PBTB, washed in PBS (pH 8.2), and incubated with secondary and tertiary layers as follows. For Ig:Ig:5 sandwiches, sections were incubated (1 hr) with goat anti-mouse IgG conjugated with 5-nm gold particles (1:50 dilution) in PBTB. For Ig:Ig:Ig:Au sandwiches, sections were incubated (1 hr) with rabbit anti-mouse IgG (1:50 dilution) in PBTB, rewashed, and incubated (1 hr) with goat anti-rabbit IgG conjugated with 5-, 10-, or 15-nm gold particles (1:50 dilution) in PBTB. For Ig:Ig:pA:Au sandwiches,

sections were incubated (1 hr) with rabbit anti-mouse IgG (as above), rewashed, and incubated (1 hr) with protein A conjugated with 5- or 9-nm gold particles (1:100 dilution) in PBTB without Tween. After binding gold particles, sections were washed in PBS and then with water, dried, and contrasted with a saturated solution of uranyl acetate in 70% ethanol. Sections were observed in a Zeiss 912 Omega electron microscope (accelerating voltage 80 kV) and images collected using a CCD camera (1024 × 1024 chip; depth 14 bits).

For Figure 4, polystyrene beads (diameter 1 μm) coated with biotin (Sigma; Poole, Dorset, UK) were embedded in 2% agarose (type VII; Sigma), dehydrated in ethanol, embedded in LR White (polymerization 5 hr at 56C), and ultrathin sections immunolabeled using one to three layers as described above. For one layer, the first antibody was goat anti-biotin conjugated with 5- or 10-nm particles (1:100 dilution). For two layers, the first antibody was goat anti-biotin (1:100 dilution) and the second rabbit anti-goat IgG conjugated with 10-nm particles (1:50 dilution). For three layers, the first was goat anti-biotin (1:100 dilution), the second rabbit anti-goat IgG (1:50 dilution), and the third protein A conjugated with 9-nm particles (1:100 dilution).

Image Analysis

Images such as those in Figure 1 were analyzed as follows (Williams 1977), using EasiVision SIS software supplied with the microscope and Excel: (a) collection of images of >60 clusters; (b) measurement of major, 2x, and minor, 2y (orthoganol), axes of each cluster and the area and perimeter of each cluster; (c) calculation of cluster diameter, D, from $D = 2\sqrt{(xy)}$, and mean cluster diameter, $\bar{D}$ from the number of clusters (N) and the diameter of individual clusters (D_1, D_2,...D_N) using

$$\bar{D} = \frac{\pi}{2}\left(\frac{N}{\frac{1}{D_1} + \frac{1}{D_2} + \cdots \frac{1}{D_N}}\right)$$

(d) calculation of the "shape factor" of clusters from 4π (area/perimeter^2). Values lay between 0.64–0.79, indicating that the underlying structures were close to spheres (which have a value of 1); (e) measurement of positions of individual particles in a cluster, the center of gravity of the cluster, and distance to nearest neighbors. [Note that use of the "new" stereology here is inappropriate because the structures analyzed have diameters less than the section thickness (for review see Royet 1991).] Numbers of particles per μm along the periphery of the plastic bead were also measured with SIS software using images like those in Figure 4.

Results

The Problem

Figure 1A illustrates the problem we wish to solve. HeLa cells were fixed and embedded in LR White. After preparation of conventional ultrathin sections, sites on the surface of sections that contained SR antigens were indirectly immunolabeled with gold particles. The immunolabeling sandwich contained a primary anti-SR antibody, a secondary immunoglobulin (Ig), and a third Ig conjugated with 10-nm gold particles. For convenience, we call such a sandwich Ig:Ig:Ig:10. [The corresponding three-layer sandwich containing protein A conjugated with a 9-nm gold particle will be called Ig:Ig:pA:9.] Immunolabeling gold particles are found in clusters over the nucleus. We define a cluster as a group of ≥2 particles lying within 40 nm of each other for quantitative analysis. Some electron-dense material underlies the clusters. This is not seen without immunolabeling and is due to the high concentration of protein in the immunolabeling sandwich. Ideally, we wish to deduce the true diameter of the underlying structures containing SR antigens by analyzing the clusters of gold particles. In practice, we do not even know whether the observed diameter of the clusters is smaller or larger than the true diameter, and we would like to obtain some estimate of the error. We will assume here that the true diameter is 50 nm (see Discussion).

The primary antibody used to detect SR sites is a mouse IgM. This primary antibody can be detected using a secondary antibody raised against either an IgM or an IgG (because such antibodies crossreact with IgMs). In principle, an anti-IgM should give higher detection levels than a crossreacting anti-IgG. However, in practice, two experiments showed that detection levels were equivalent. In the first, the primary anti-SR antibody was adsorbed onto a grid and immunodetected using 10-nm gold particles conjugated either to an anti-IgM or an anti-IgG. The two secondary antibodies gave equivalent labeling intensities (not shown). In the second experiment, SR sites in sections were detected using the two secondary antibodies, again with equivalent results (Table 1; compare Methods 4 and 5). Therefore, we used an anti-IgG as the second antibody for most experiments, because results obtained with it are of wider interest.

SR clusters like those seen in Figure 1A have major and minor (orthoganol) axes of 61 ± 13 nm and 51 ± 11 nm (Table 1). Because sections are cut randomly, few underlying structures present profiles with maximal diameters to the immunolabeling probe. We can calculate a maximal diameter of 64 nm by correcting for this "Holmes" effect using standard stereological methods, if we assume that the underlying structures have similar major and minor axes (see Materials and Methods; reviewed by Williams 1977).

The Effect of Number of Immunolabeling Layers and Particle Size

Because the estimated diameter was larger than the assumed diameter of the structure, we must correct for particle size and probe length. Therefore, we investigated the effects of reducing both, and typical ex-

Table 1 Effect of different labeling methods on size of clusters marking SR sites[a]

Method[b]	Particles per cluster	Distance to nearest neighbor in cluster (nm)	Cluster		Calculated diameter (nm)
			Major axis (nm)	Minor axis (nm)	
1. Ig:Ig:5	6 ± 3	17 ± 3	49 ± 11	39 ± 8	50
2. Ig:Ig:Ig:5	10 ± 4	16 ± 7	51 ± 10	43 ± 9	54
3. Ig:Ig:pA:5	9 ± 3	14 ± 7	56 ± 19	45 ± 16	61
4. Ig:Ig:Ig:10	11 ± 5	17 ± 4	61 ± 13	51 ± 11	64
5. Ig:Ig:Ig:10	9 ± 4	17 ± 5	58 ± 13	48 ± 7	62
6. Ig:Ig:pA:9	10 ± 3	16 ± 5	70 ± 14	58 ± 11	76
7. Ig:Ig:Ig:15	8 ± 2	22 ± 5	71 ± 14	60 ± 13	77

[a]SR antigens on the surface of sections were immunolabeled with 1–3 layers of immunoglobulins (Ig) ± protein A (pA) and gold particles of 5–15 nm (as in Figure 1), before the numbers and distances (± SD) between (and within) clusters were measured. The diameter of the cluster was calculated using standard stereological procedures (see Materials and Methods).
[b]A secondary anti-Ig(Fc) was used, except for Method 5 (in which a secondary anti-IgM was used instead).

amples are illustrated in Figures 1B–1G. Reducing particle size slightly reduced cluster diameter; extrapolation back to zero particle size (for both Ig:Ig:Ig:Au and Ig:Ig:pA:Au sandwiches) gave cluster diameters of 42 nm (Figure 2). The slope of the line for Ig:Ig:Ig:Au indicates that particle diameter is directly related to cluster diameter, with a reduction in particle diameter by 5 nm reducing cluster diameter by ~10 nm (consistent with a reduction of 5 nm on each side). However, reducing the number of immunoglobulins bridging antigen and gold particle from three to two had less of an effect (consistent with a reduction of only 2 nm on each side) (Figure 1E; Table 1). Unfortunately, use of only one immunoglobulin in the bridge gave too little labeling for accurate analysis (not shown, but see below). Perhaps surprisingly, replacing the last immunoglobulin (length ~9 nm) with a shorter protein A (pA) molecule (diameter ~5 nm) (Harlow and Lane 1988) slightly increased cluster diameter (Figures 1F and 1G; Table 1).

When we used protein A, we noticed that gold particles were often peripherally distributed in a cluster (Figures 1F and 1G). Images gave the impression that long immunolabeling complexes had first bound to clustered antigens on the surface of the grid before they fell outwards to leave a circle of gold particles around the edge. Quantitative analysis confirmed this peripheral distribution (Figure 3). The position of each of 600 particles was measured relative to the center of gravity of a cluster; these relative positions are plotted in Figure 3. Ig:Ig:Ig:10 complexes gave a uniform distribution in both a scatter plot and a histogram, in which particle densities in successive 4-nm rings were plotted (Figure 3B). However, Ig:Ig:Ig:5 complexes showed a slight tendency to be located peripherally (Figure 3A), whereas complexes containing protein A were obviously concentrated there (Figures 3C and 3D).

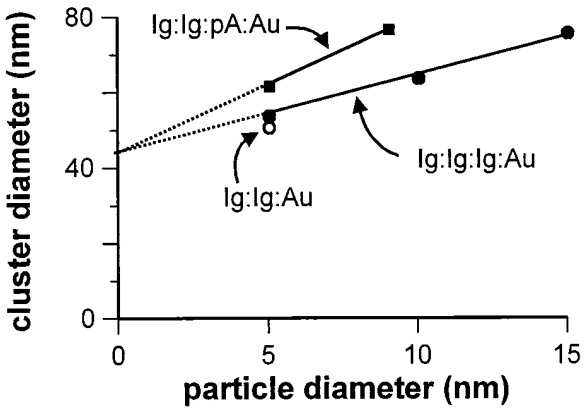

Figure 2 The effect of diameter of gold particles on cluster diameter (corrected for the "Holmes" effect). SR antigens were immunolabeled (as in Figure 1) using the layers and gold particles indicated.

Immunolabeling Particles Are Tightly Packed

A protein coat surrounds the gold particle used in the final layer of an immunolabeling sandwich. In general, protein A gives a thicker coat than an immunoglobulin, small particles are surrounded by thicker layers, and thickness depends on the protein concentration present during binding. For the size of particles used here, layers are 3–6 nm thick (Lea and Gross 1992). As a result, a 5-nm particle is coated with an immunoglobulin layer of ~6 nm, giving an effective diameter of 17 nm. If such a coated particle is tightly packed in a cluster, the center-to-center distance will be 17 nm. This is the distance between nearest neighbors in SR clusters (Table 1).

Effect of Layers on Sensitivity

Both logic and the above results suggest that it is sensible to use the smallest probe possible (i.e., one immunoglobulin conjugated with a small gold particle). In practice, however, increased resolution comes at the price of reduced sensitivity (Bendayan 1995). We demonstrated this using a different system because the

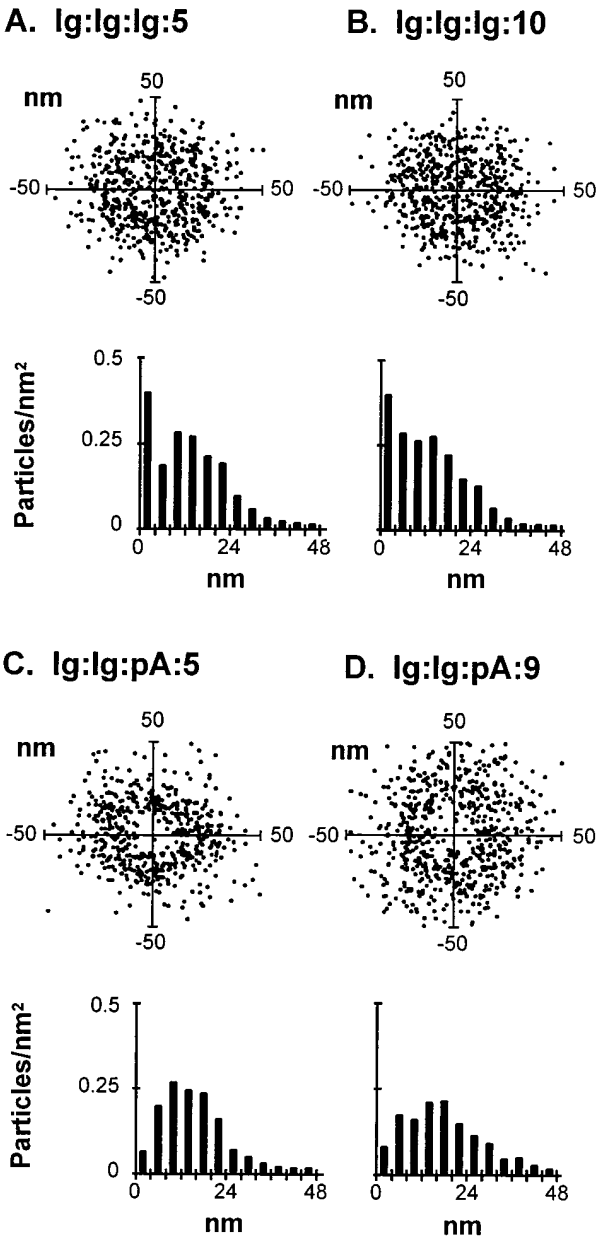

Figure 3 Distributions of 600 particles relative to cluster center. SR antigens were immunolabelled (as in Figure 1) using (**A**) Ig:Ig:Ig:5, (**B**) Ig:Ig:Ig:10, (**C**) Ig:Ig:pA:5, and (**D**) Ig:Ig:pA:9. The same data are shown using scatter plots or histograms giving particle densities in successive 4-nm rings. Protein A gives few particles in the center of clusters.

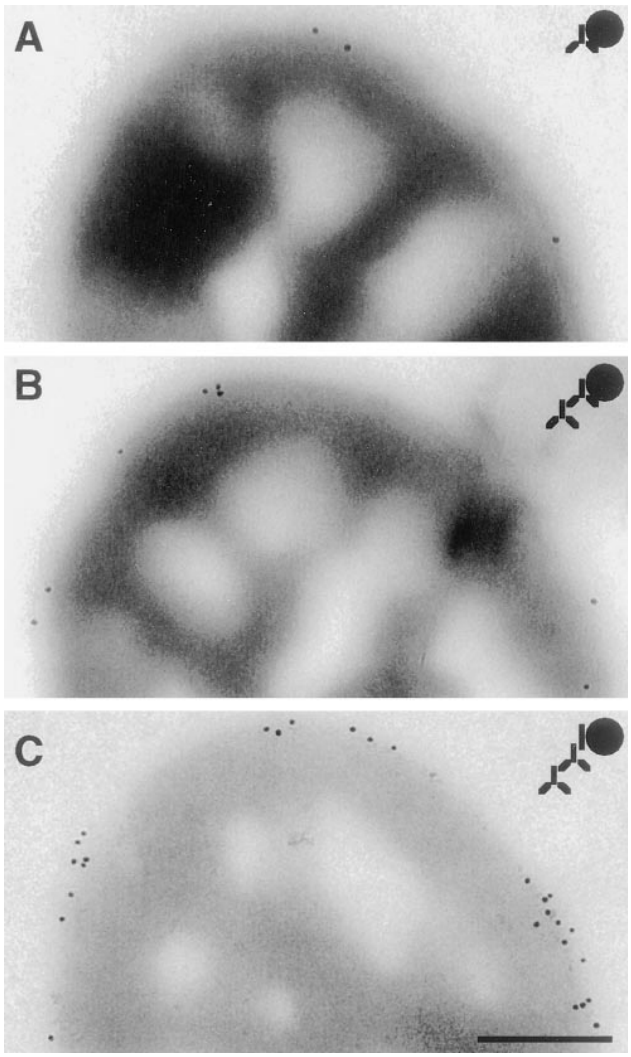

Figure 4 Effect of the number of layers in the immunolabeling sandwich on labeling intensity. Polystyrene beads (diameter 1 μm) coated with biotin were immunolabeled with 10-nm gold particles using (**A**) anti-biotin conjugated with gold, (**B**) anti-biotin followed by anti-mouse conjugated with gold, and (**C**) anti-biotin followed by rabbit anti-mouse and then protein A–gold. As the number of immunolabeling layers increases, both labeling intensity and particle clustering increase. Bar = 200 nm.

appropriate antibodies were available. Polystyrene beads (diameter 1 μm) coated with biotin were embedded in LR White and the surfaces of sections labeled with 10-nm gold particles using one, two, or three layers in the sandwich. In each case, antibody dilutions were used that gave maximal labeling. Increasing the number of layers increases both labeling intensity and the percentage of particles in clusters (Figure 4; Table 2). Using 10-nm particles, one layer gave only 2 particles/μm along the perimeter of the bead, presumably because the large gold conjugate has little access to biotin in surface crevices. A small reduction in size of the conjugate by inclusion of a 5-nm particle marginally increases labeling intensity (to 2.5 particles/μm). With two layers and 10-nm particles, the smaller size of the first antibody permits greater access and almost triples labeling, while the amplification allowed by three layers increases it eightfold. This amplification was reflected by an increase in the percentage of particles in clusters, as two or more particles can now mark one epitope.

Table 2 Effect of the number of layers in the immunolabeling sandwich on detection[a]

	5 nm		10 nm	
Layer	Particles/μm	% in clusters	Particles/μm	% in clusters
1	2.5 ± 0.7	20	2.0 ± 1.1	26
2	nd	nd	5.7 ± 1.3	28
3	nd	nd	16 ± 4.0	90

[a]Polystyrene beads (diameter 1 μm) coated with biotin were embedded in LR White, sectioned, and immunolabeled with 5- or 10-nm gold particles using one, two, or three layers in the sandwich. After collecting images such as those in Figure 4, the number of particles per μm along the perimeter of the bead (± SD) and the percentage of particles lying within 40 nm of one another (i.e., in clusters) were measured. nd, not done.

Discussion

Problems Associated with Determining the Size of SR Sites by Immunolabeling

SR sites are defined using an MAb that recognizes a phosphorylated subset of the SR family of proteins (Roth et al. 1990). Indirect immunogold labeling with this antibody reveals many small clusters of ~10 gold particles on the surface of ultrathin sections; these clusters typically have a major axis of ~60 nm (Iborra et al. in press). Our main purpose was to gauge the error in estimating the diameter of the underlying SR site, using the diameter of the overlying cluster of gold particles as a guide. Because sections are cut randomly, few underlying structures present profiles with maximal diameters to the immunolabeling probe. After correction for this "Holmes" effect (Williams 1977), SR sites were found to have diameters of 50–77 nm, which depended on the type of immunolabeling probe (Table 1). Because a probe such as Ig:Ig:Ig:10 is so long, it was formally possible that cluster diameter was overestimated by twice the probe length (Figure 5A). Alternatively, if gold particles lie more directly over the antigen they mark (as in Figure 5B), cluster diameter would reflect true diameter more accurately. Moreover, the low number of particles in a cluster might even lead to an underestimate. Consider, for example, a case in which a primary (divalent) antibody remains stably bound only if attached through both binding sites to target antigens. Inevitably, then, the maximal diameter of the cluster will be less than that of the underlying structure (Figure 5F). For reasons such as these, we did not know whether the diameter of the cluster of gold particles was larger or smaller than that of the underlying SR site.

The True Size of SR Sites

Most SR sites are easily extracted from nuclei (Iborra et al. in press), and they can then be isolated on sucrose gradients as large nuclear ribonucleoprotein particles of ~200 S (Sperling et al. 1997). A low-resolution structure of these isolated particles shows that they are tetramers with overall diameters of ~50 nm

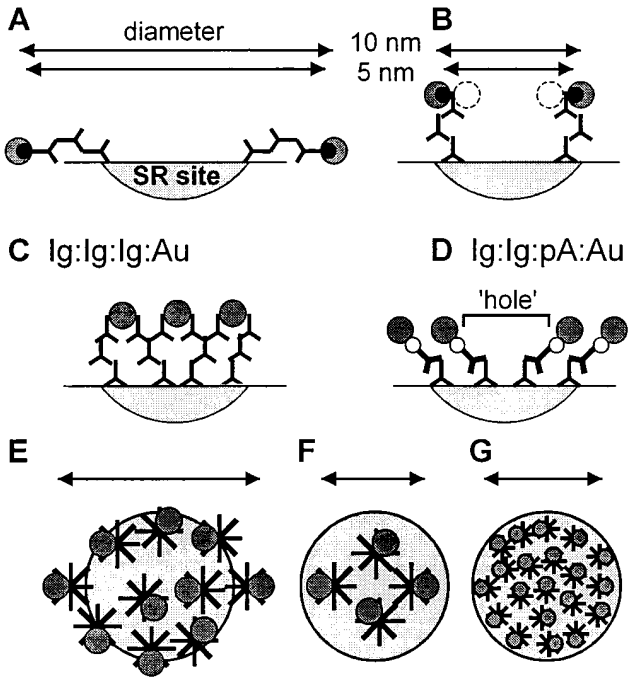

Figure 5 Factors affecting cluster diameter (**A–D** side views; **E–F** plane views). Gold particles of 5 or 10 nm (light and dark gray circles) are attached through Igs (Y-shaped structures) ± protein A (open circles) to antigens in an SR site. The primary antibody used was an IgM; for the sake of simplicity, only one of its five subunits is drawn. The secondary antibody, in our case an anti-IgG(Fc), would probably bind to only one Fc site at the center of the primary IgM, as shown. (**A**) An extreme case, in which cluster diameter is overestimated by twice the length of the sandwich (i.e. Ig:Ig:Ig:Au). Ten nm particles yield a diameter that is 10 nm greater than that given by 5-nm particles. (**B**) Another possibility giving a shorter diameter. Because the center is more crowded than the periphery, peripheral particles tend to be on the outside (as shown) rather than the inside (dotted circles). Then, 10-nm particles also give a greater diameter than 5-nm particles. Here, reducing the number of Igs in the sandwich from three to two has no effect on cluster diameter (unlike **A**). (**C**) A truer representation of Ig:Ig:Ig:10 complexes over a site. Because Igs are bivalent and each particle is associated with many Igs, particles are usually attached through >1 Ig. (**D**) A particle coated with protein A has fewer binding sites and so will be attached through fewer protein bridges. Therefore, particles may collapse during drying towards the periphery (leaving a central "hole"). (**E–G**) Viewed from above, a complex like that in **B** (drawn here as a gray gold particle overlying Igs) may overlap the edge of the site, so the measured diameter is greater than the true diameter (**E**). If complexes cannot overlap (perhaps because both sites in the first Ig must bind), diameter is underestimated (**F**), although maximal packing of many smaller complexes gives a truer estimate of diameter (**G**).

(Yitzhaki et al. 1996; Sperling et al. 1997). What is the true diameter of these sites in vivo? Unfortunately, we can only guess at the answer. Several factors make an accurate estimate impossible. We compare diameters in structures visualized indirectly by two different procedures: after immunolabeling structures embedded in ultrathin LR White sections (Iborra et al. 1996; and this work) or after isolation and negative staining (Yitzhaki et al. 1996; Sperling et al. 1997). Both pro-

cedures probably distort structure. For example, many tissues and virus particles shrink by ≤30% when dehydrated, a necessary part of both procedures (for reviews see Hayat 1989; Hayat and Miller 1990; Mollenhauer 1993), and negative staining can flatten isolated structures, increasing their diameter (reviewed by Hayat and Miller 1990). The scale of such effects will be illustrated with two examples. Small-angle X-ray diffraction shows that hydrated virions of bacteriophage T7 have diameters of ~60 nm, but negative staining can reduce this by ~8% as virions first shrink and then expand (Serwer 1977). Cryoelectron microscopy shows that intracellular mature virions of *Vaccinia* virus appear as smooth, rounded rectangles about 360 × 270 nm, but negative staining reveals structures that are as long but ~17% narrower (Dubochet et al. 1994). An additional and probably important factor makes it difficult to compare sizes in situ and after isolation. Removing SR sites from their native state in the nucleus would be expected to alter their size. Bearing in mind these reservations, we will assume here that SR sites found in nuclei have a true diameter of 50 nm.

To establish the true diameter of SR sites, we determined how variations in the number of immunoglobulin (or protein A) molecules in the immunolabeling sandwich, and the size of the gold particle, affected cluster diameter. We can draw several conclusions from these studies.

First, as expected, reducing particle size reduces cluster diameter (Figures 5A and 5B). Extrapolation back to zero particle size (for both Ig:Ig:Ig and Ig:Ig:pA sandwiches) gives cluster diameters of ~42 nm (Figure 2). This value is less than the 50 nm measured by negative staining, perhaps because of effects such as those illustrated in Figure 5F. A reduction in particle diameter by 5 nm reduces cluster diameter by ~10 nm; this is consistent with a reduction of 5 nm on each side, and so with the model in Figure 5A. Then, we would expect that reducing the number of molecules bridging antigen and gold particle would also reduce cluster diameter, but it had little effect (Figures 1F and 2). However, the two results can be reconciled if complexes tend to be arranged as in Figure 5B, with peripheral particles on the outside of peripheral immunolabeling complexes.

Second, reducing the number of immunoglobulins in the immunolabeling sandwich from three to two reduced cluster diameter by ~4 nm (Table 1).

Third, under our conditions immunolabeling particles are tightly packed. A protein "halo" of 3–6 nm surrounds the gold particle used in the final layer of the sandwich; halo thickness is inversely related to particle size, with protein A forming a thicker coat than an immunoglobulin (Lea and Gross 1992). As a result, a 5-nm particle has an immunoglobulin halo of ~6 nm, giving an effective diameter of 17 nm. Tight packing then gives a center-to-center distance of 17 nm, which is the distance seen (Table 1). As expected, this distance becomes shorter with protein A and larger particles (Table 1). If we assume tight packing, we can calculate from the data in Table 1 that both immunoglobulin and protein A halos around particles of 9–15 nm are 3.5 nm, the expected value. The organization illustrated in Figure 5B (but not that in Figure 5A) gives this kind of tight packing (as in Figure 5C).

Fourth, and perhaps surprisingly, replacing the last immunoglobulin (length ~9 nm) in the sandwich with a protein A molecule (diameter ~5 nm) slightly increases cluster diameter (Figures 1G and 1H; Table 1). With protein A, gold particles are often concentrated at the periphery (Figures 1G, 1H, and 3), as if long complexes fall outwards after binding. This can be explained by the lower valency of protein A–gold complexes. Although an individual immunoglobulin and protein A molecule have roughly equivalent numbers of binding sites when bound to a gold particle (Harlow and Lane 1988), each particle is coated by twice as many immunoglobulins molecules (Ghitescu and Bendayan 1990). Thus, a 10-nm particle is coated with 12–20 immunoglobulin molecules and a 9-nm particle with only 7–11 protein A molecules (Ghitescu and Bendayan 1990). As a result, protein A–gold has a lower overall valency and will be attached through fewer protein bridges to the surface of the grid. Therefore, it is probably more prone to collapse than immunoglobulin–gold, which is more heavily crosslinked (Figure 5CD).

Fifth, and as expected, increasing the number of layers in the sandwich increases sensitivity (Figure 4; Table 2). Unfortunately, four layers generally give too high a background for general use, and one layer, which should give the highest resolution, is not sufficiently sensitive to give acceptable levels of labeling (not shown).

Which is the best approach to use to determine the diameter of an SR site? Clusters of Ig:Ig:5 complexes fortuitously give a diameter of 50 nm (Table 1), which we assume is the correct one (but see above). In practice, the higher sensitivity of three-layered sandwiches is required to detect most sites, whereas larger particles of 9 or 10 nm are more easily seen at a conveniently low magnification.

Corrected Diameters and Numbers of SR Sites

Using Ig:Ig:pA:9, we found previously that SR sites had diameters of 76 nm (Iborra et al. in press). If the diameter of an SR site is truly 50 nm, this means that we overestimated diameter by ~50%. We also calculated the total number of sites in 3-D space (using standard stereological procedures) from the numbers

and diameters of clusters seen in 2-D sections, with knowledge of nucleoplasmic volume (e.g., Iborra et al. 1996). However, a 50% overestimate of the radius of a spherical object leads to a 50% underestimate of the numbers of that object in a nucleus. Therefore, we must revise our previous estimate of the number of SR sites in a nucleus from 45,000 to 68,000. An analogous correction to the diameter of a transcription "factory" (i.e., from 82 nm to 56 nm) would increase the factory number from 2400 to 3600 (Jackson et al. in press).

Acknowledgments

Supported by the Wellcome Trust.
We thank Jeremy Sanderson for his help.

Literature Cited

Bendayan M (1995) Colloidal Gold Post-embedding Immunocytochemistry. Stuttgart, Gustav Fischer-Verlag

Dubochet J, Adrian M, Richter K, Garces J, Wittek R (1994) Structure of intracellular mature vaccinia virus observed by cryoelectron microscopy. J Virol 68:1935–1941

Ghitescu L, Bendayan M (1990) Immunolabeling efficiency of protein A–gold complexes. J Histochem Cytochem 38:1523–1530

Griffiths G (1993) Fine Structure Immunocytochemistry. Berlin, Heidelberg, Springer-Verlag

Harlow E, Lane D (1988) Antibodies: a Laboratory Manual. Cold Spring Harbor, NY, Cold Spring Harbor Laboratory Press

Hayat MA (1989) Principles and Techniques of Electron Microscopy: Biological Applications. 3rd ed. Boca Raton, FL, CRC Press

Hayat MA, Miller SE (1990) Negative Staining. New York, McGraw–Hill

Iborra FJ, Pombo A, Jackson DA, Cook PR (1996) Active RNA polymerases are localized within discrete transcription 'factories' in human nuclei. J Cell Sci 109:1427–1436

Iborra FJ, Jackson DA, Cook PR (1998) The path of transcripts from extra-nucleolar synthetic sites to nuclear pores: transcripts in transit are concentrated in discrete structures containing SR proteins. J Cell Sci, in press

Jackson DA, Iborra FJ, Manders EMM, Cook PR (1998) Numbers and organization of RNA polymerases, nascent transcripts and transcription units in HeLa nuclei. Mol Biol Cell, in press

Kramer A (1996) The structure and function of proteins involved in mammalian pre-mRNA splicing. Annu Rev Biochem 65:367–409

Lea P, Gross DK (1992) Effective diameters of protein A–gold and goat anti-rabbit–gold conjugates visualized by field emission scanning electron microscopy. J Histochem Cytochem 40:751–758

Mollenhauer HH (1993) Artifacts caused by dehydration and epoxy embedding in transmission electron microscopy. Microsc Res Tech 26:496–512

Roth MB, Zahler AM, Gall JG (1990) A monoclonal antibody that recognizes a phosphorylated epitope stains lampbrush chromosomes and small granules in the amphibian germinal vesicle. J Cell Biol 111:2217–2223

Royet J-P (1991) Stereology: a method for analyzing images. Prog Neurobiol 37:433–474

Serwer P (1977) Flattening and shrinkage of bacteriophage T7 after preparation for electron microscopy by negative staining. J Ultrastruct Res 58:235–243

Sperling R, Koster AJ, Melamed–Bussudo C, Rubinstein A, Angenitzki M, Berkovitch–Yellin Z, Sperling J (1997) Three-dimensional image reconstruction of large nuclear RNP (lnRNP) particles by automated electron tomography. J Mol Biol 267:570–583

Williams M (1977) Quantitative methods in biology. In Glauert AM, ed. Practical Methods of Electron Microscopy. Vol 6. Amsterdam, North-Holland, 48–69

Yitzhaki S, Miriami E, Sperling R, Sperling J (1996) Phosphorylated ser/arg-rich proteins: limiting factors in the assembly of 200S large nuclear ribonucleoprotein particles. Proc Natl Acad Sci USA 93:8830–8835

Zahler AM, Lane WS, Stolk JA, Roth MB (1992) SR proteins: a conserved family of pre-mRNA splicing factors. Genes Dev 6:837–847